Proceedings of the 12th International Conference on Fluid Flow, Heat and Mass Transfer (FFHMT 2025)
July 15, 2025 - July 17, 2025 | Imperial College London Conference, London, United Kingdom
Paper No. 226
DOI: 10.11159/ffhmt25.226

Enhancing Performance of District Heating Systems Using CO_2 as a Working Fluid by Operation Optimization

Meisam Sadi[1], Rikke C. Pedersen[1], Jakob Worm[2], Robert Pratter[3], Ahmad Arabkoohsar[1]
[1]Technical University of Denmark
Lyngby, Denmark
[2]PlanEnergi, Aarhus, Denmark
[3]4ward Energy Research GmbH, Graz, Austria
meisa@dtu.dk

Abstract
CO_2-based district energy systems offer an up-and-coming alternative to water-based district energy systems due to the potential for lower investment costs, smaller components, and improved efficiency compared to traditional water-based systems. The heating system investigated in this study relies on a CO_2-based district energy system, considering a heat pump in the central station for extracting heat from the ambient, while heat pumps in the consumer substations provide the required heating for the end users. The system performance is influenced by temperature throughout the cycle's operation. The purpose of this study is to find the optimal operating conditions of the network considering variations in the ambient temperature and demand profile throughout the year. Based on optimal operation of the system, a 4 % reduction in operation costs appears when compared to the benchmark system. The reduction of operational costs would enhance the economic feasibility of such projects.

Keywords**:** CO_2 district heating system, operational cost, optimization, heat pump.

1. Introduction

The transition towards sustainable district energy systems will reduce greenhouse gas emissions and help combat climate change [1]. These systems can increase energy efficiency by optimally using renewable energy sources and heat recovery [2]. Developing sustainable regional energy systems can help reduce energy costs and improve energy security for citizens, as well as reduce dependence on fossil fuels and create a cleaner and healthier environment for future generations. However, the design and operation of these systems must be carefully chosen to ensure optimal performance.

Traditional district energy systems use water in pipelines to carry energy from the production site to the consumer. Water is an abundant, non-toxic, and cheap resource. However, it is prone to freezing in cold regions, has a corrosive nature, and the water hardness can cause severe fouling. This can damage pipes and equipment and thereby reduce the performance of district energy systems. Another issue in traditional district energy systems, especially for delivering heat, can be energy losses to the surroundings during the energy transport [3]. Using alternative working fluids instead of water can increase thermal efficiency and reduce energy losses [4]. Some working fluids may have better thermodynamic properties that allow the use of lower or higher temperatures and enhance system efficiency. Selecting the right fluids can reduce problems such as freezing, corrosion, and scaling, as well as maintenance and operating costs.

Carbon dioxide (CO_2) as a working fluid in district energy systems can improve the investment costs of the piping system compared to water. It utilizes the latent heat of vaporization of the working fluid rather than sensible heat, which allows for the design of smaller and more efficient components [5]. CO_2 has favorable thermodynamic properties that increase the efficiency of heating and cooling systems and reduce energy consumption [6]. Utilization of carbon dioxide instead of water can pave the way for a reduction in problems such as freezing, corrosion, and scaling, and reduce maintenance and operating costs. Studying CO_2-based district heating networks can help develop new and more sustainable technologies in the field of urban energy [4]. These systems can play an important role in reducing greenhouse gas emissions and combating climate change, which is in line with the global sustainable development goals.

Different aspects of using CO_2 as the working fluid in district heating systems have not been covered in the literature and thus need to be addressed. Therefore, this study focuses on a geographically limited district heating system utilizing CO_2

as the working fluid. The purpose of the study is to optimize key operating parameters and to understand how these impact the profitability of the system. This paper aims to find the optimal operating conditions of the network considering variations in the ambient temperature and demand profile throughout the year. The results will be useful for comparing the performance of the CO_2-based system with conventional systems, and to further develop CO_2-based systems providing both heating and cooling.

2. Methodology

In this section, the methodology is explained, the system is introduced, and the approach is described.

2.1 System Description

Fig. 1 illustrates the system under investigation. When heating is supplied to a consumer station, CO_2 vapor is extracted from the main gas pipeline and sent through a substation. Heat is transferred from the CO_2 network to the building's internal loop, which causes the CO_2 to condense. Then, liquid CO_2 is pumped into the liquid line. The CO_2 then enters the main liquid pipeline. This pipeline leads to the central station, where heat is absorbed by CO_2 to maintain the energy balance of the network. At the central station, the liquid CO_2 is vaporized. Two heat sources were considered for the central heat pump. Initially, it was assumed to utilize the ambient air with temperature variations throughout the year, while a case using a nearby lake at constant temperature throughout the year was also considered.

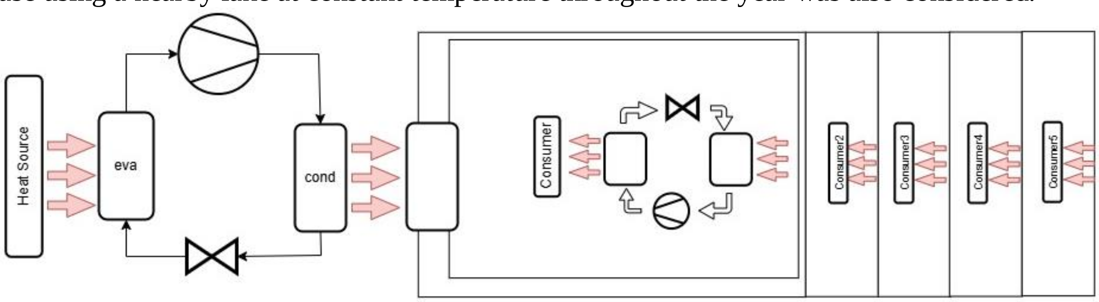

Fig. 1: CO_2-based district heating network schematic, main components, and flow direction.

2.2 Algorithm Description

First, initial guess values are defined for the network parameters, including the maximum pressure increase of the network and the pressure drop in the liquid and vapor lines. Then the initial guess values for temperature, enthalpy, and mass flow rate of the network's pipes are calculated. The nominal pipe size standard is used to define the right size of each pipe and the diameter of the pipes based on the design velocity of the vapor and liquid pipelines [4], [6]. The inlet pressure of each pipeline and the flow rate of the vapor or liquid inside the pipelines are calculated output variables. After determining the diameter of the pipeline, the actual velocity of fluid, the installation depth of the pipe within the soil, the specification of the soil, the inlet temperature and pressure, and the flow rate, we proceed to compute the outlet pressure and temperature, the pressure drop, and the heat transfer between the pipe and the environment. In this process, the outlet of the first pipe is defined as the inlet of the second pipe. Here, based on the initial guess values, the network properties are defined. It has to be ensured that the temperature of the return liquid in the first consumer, which is taking the heat from the central station, is equal to the network temperature. In this process, the working fluid undergoes heating in the central station to reach a certain degree of superheat. The calculation process iteratively solves the system of equations until the specified conditions are met, and it is ensured that the fluid in the vapor and liquid lines remains within a single phase in the pipes.

2.3 Governing Equations

In the upcoming section, we'll present the governing equations for the proposed system. By treating each element as a control volume, the governing equations can be illustrated in a general way. Central and consumer heat pumps are modeled using a coefficient of performance (COP). The Lorenz efficiency (based on the defined value in [7]) is used to relate the performance of the heat pumps to different operating temperatures. In the central heat pump, the average entropic temperature of the district heating water and the condensation/evaporation temperature of CO_2 at the central station are used. For consumer heat pumps, the temperature of the fluid in the network and the circulating coolant are used. The assumed temperatures and isentropic efficiencies of the pumps are given in Table 1.

$$\mathrm{COP_{cen}} = \eta_{\mathrm{cen,Lorenz}}\mathrm{COP_{Lorenz}} = \eta_{\mathrm{cen,Lorenz}}\left(\frac{\overline{T}_{\mathrm{H}}}{\overline{T}_{\mathrm{H}} - T_{\mathrm{C}}}\right) \tag{1}$$

The vapor line temperature is regulated according to the temperature requirement of the end user. The heat transfer between the pipe and the environment is modeled in simulations according to the long-term conditions of the system and the pressure drop in the pipes. The friction of the pipes is modeled by the Reynolds number and the roughness of the inner surface of the pipe.

$$\frac{1}{\sqrt{f}} = -2\log\left(\frac{\varepsilon_{\mathrm{rel}}}{3.71} + \frac{2.51}{\mathrm{Re}\sqrt{f}}\right) \text{ with } \varepsilon_{\mathrm{rel}} = \frac{\varepsilon_{\mathrm{abs}}}{D_{\mathrm{i}}} \tag{2}$$

The pressure drop and friction are integrated with the fluid velocity, length and diameter of the pipe according to the following equation:

$$\Delta p = \frac{1}{2}\rho u^2 f \frac{L}{D_i} \tag{3}$$

In long networks, the pipes are buried in the soil and there is a possibility of heat loss or gain. The heat transfer coefficient is used to identify the amount of heat transfer between the pipe and the environment.

$$\dot{Q}_{\mathrm{amb}} = UA\Delta T \text{ with } \Delta T = \frac{(T_{\mathrm{amb}} - T_{\mathrm{in}}) + (T_{\mathrm{amb}} - T_{\mathrm{out}})}{2} \tag{4}$$

The total thermal resistance is the inverse of the heat transfer coefficient and is calculated based on the soil resistance and other factors.

$$UA = \frac{1}{R_{\mathrm{tot}}} \tag{5}$$

$$R_{\mathrm{tot}} \approx R_{\mathrm{soil}} = \frac{1}{S_f k_{\mathrm{soil}}} \text{ with } S_f = \frac{2\pi L}{\ln(4z/D_{\mathrm{o}})} \tag{6}$$

To design the dimensions of the pipes, the maximum allowable flow rate and pressure are taken into account. The diameter of the pipes is chosen so that the CO_2 flow does not exceed the allowable velocity.

$$t = \frac{p_{\mathrm{max}} D_i}{2\sigma_{\mathrm{max}}} \tag{7}$$

The maximum allowable material stress must not exceed the limits set in Directive 2014/68/EU.

$$\sigma_{\mathrm{max}} = \mathrm{Min}\left(\frac{2}{3}\sigma_{\mathrm{y}}, \frac{5}{12}\sigma_{\mathrm{t}}\right) \tag{8}$$

The objective function is defined as the total electricity price.

$$TEP = \sum_{i=1}^{N} Total \text{ Electricity Price} \tag{9}$$

2.4 Consumers, Demand, and Temperature Profile

In this section, the information about the demand is represented. The location of the unit is Aalborg, a city in northern Denmark, with temperature profiles represented in Fig. 2 (a). For five end users located in a regional cluster, the heat demand is illustrated in Fig. 2 (b).

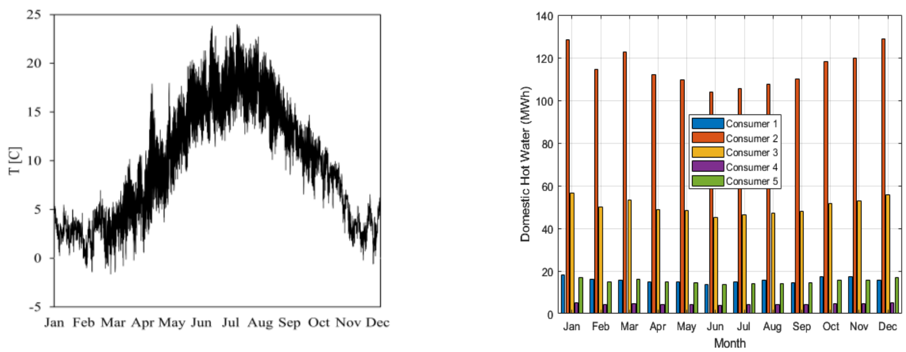

Fig. 2: Hourly temperature and monthly profile heat demand for area five consumers.

2.5 Optimization Fundamentals

The Genetic Algorithm (GA) is the optimization method used to solve this engineering problem. The structure of GA consists of the following components: Initial Population, Fitness Function, Selection, Crossover, Mutation, and Termination Criteria [8]. GA starts by generating a random set of solutions to cover the search space. Sometimes, prior knowledge is used to improve the initial solutions. Fitness function evaluates the quality of the solutions based on the objective function of the problem and guides the algorithm towards the optimum. Then, parents are selected by methods such as a roulette wheel or tournament, with priority given to solutions with higher fitness. Crossover produces new solutions by combining the characteristics of the parents. Single-point or two-point variants are applied with a probability of 0.7 to 0.9. The mutation with small random changes (probability 0.01 to 0.1) prevents getting stuck in a local optimum. Finally, the algorithm stops upon reaching a certain number of generations, convergence, or a certain value of fitness to balance accuracy and computational time.

4. Results and Discussion

In heating mode, the environment is cold (in design mode about -6 ℃), and the hot consumer side has a temperature of 60 ℃. The CO_2 network typically has a temperature between these two temperatures and could change in this range. If the temperature is close to the environment, the COP is expected to be high on the central heat pump side. A high COP of the heat pump at the central station side implies that the COP of the heat pump on the end-user side would be low. The demand of the consumer side is supplied by the CO_2 network and the energy consumed by the compressor in the heat pump, and a lower COP means that more electrical energy must be consumed in these heat pumps, but less heat needs to be received from the network. On the other hand, the COP of the central heat pump is high, meaning that the operational cost is reduced. Turning now to the second case, in which the network temperature is operated closer to the consumer's temperature demand. Thus, under this circumstance, the temperature difference between the network and the environment is large, and the COP of the central heat pump would be low. The consequence would be high electricity consumption of the central heat pump. On the consumer side, the temperature difference will be low, the COP will be high, and the consumer's electricity consumption will be low. In this case, the consumer will receive more heat from the network than in the previous case. Therefore, we need to optimize to see at what temperature heat will be received and transferred from the network.

Pareto front spread is represented in Fig. 3, displaying the solution diversity and the spreads in the objective space. In the initial generations, the Pareto Front Spread (PFS) is approximately 94, indicating that the best non-dominated individuals have objective function values spread within this range. As the generations progress, this spread decreases and reaches smaller values, reflecting improved convergence of solutions. It reduces to 70 and eventually approaches zero after 16 generations. Thus, in the final generations, the value of the objective function for the best individuals is around zero, and these individuals have reached the optimal point, and there is no difference between the members. The second figure shows the objective function landscape and displays how the objective function changes with the variation of the decision variable. The figure highlights the points where the objective functions reach their maximum or minimum values, or the ranges in which the objective functions remain constant.

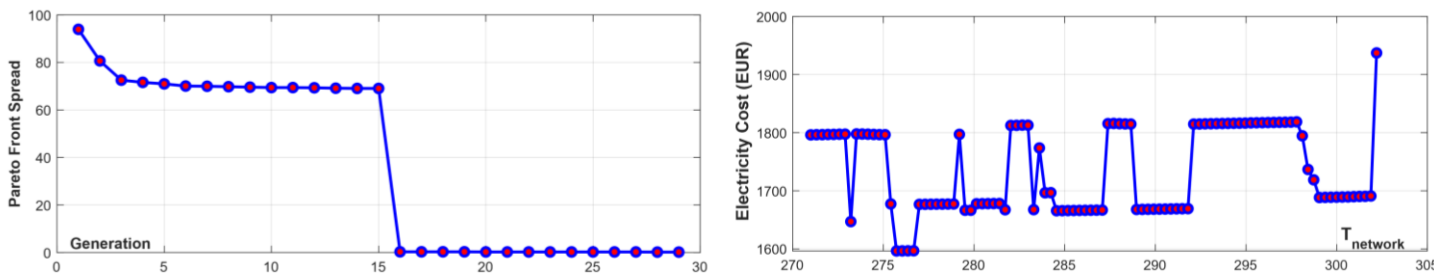

Fig. 3 Pareto front spread over generations and the variation of the objective function against the $T_{network}$ for the design point.

From the previous part of the study, the optimum temperature for the network could be calculated to be 278 K when the ambient temperature is 267 K. During the operation of the system, the temperature of the environment changes, and demand is not constant. So, for each hour of operation, the system should be adjusted for its best performance. For this reason, we should find the optimum operational point for each hour based on the ambient temperature and the hourly demand, considering that the system is previously designed, and the sizing is determined. For this condition, the optimum operation is suggested in Fig. 4. In this figure, we can see how the network's temperature is optimized. This figure shows that in this network temperature, the minimum operation cost of the network will occur. The network's temperature variation range is between -3 °C and 27.8 °C. Based on the statistical distribution vector, the most repeated optimum network temperature is found to be around 10 °C during the operation period, with the repetition of more than 1500 times. This temperature could be defined as an optimal point for the network. However, it could be observed that this temperature is not the only repeated optimum temperature, and a repetition of about 750 times is observable for the optimal temperature of 20 °C.

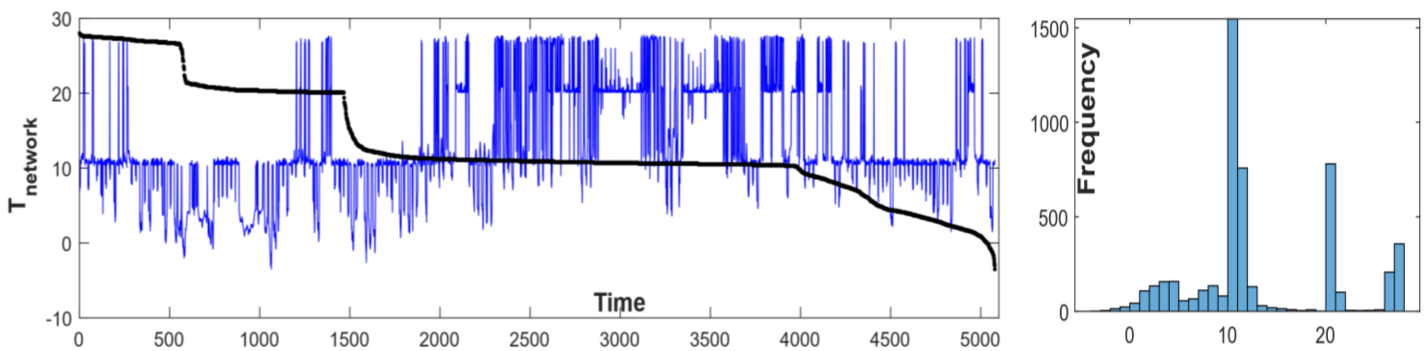

Fig. 4 Optimum network temperature and the related statistical distribution vector for the central air source heat pump.

The optimum network temperature is defined according to Fig. 4, and the system is operated for the whole period. The corresponding operational costs are represented in Fig. 5. This shows how this optimum process could impact on the system's operation and the electricity cost. As shown in this figure, the operation cost starts at 1500 USD and progressively decreases, approaching zero, for days with very low demands. Comparison to the benchmark system in that situation can show how the system is improved by the optimal process.

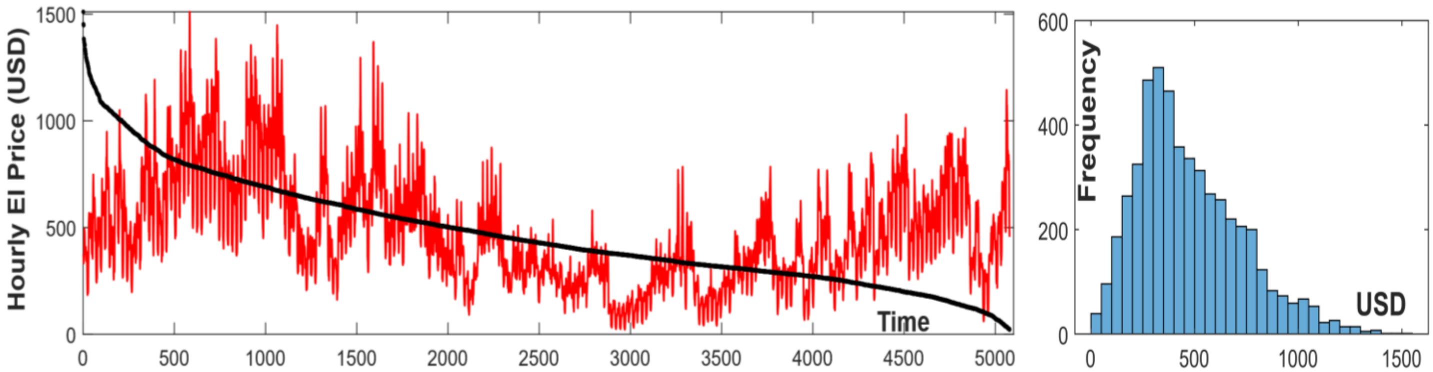

Fig. 5: Hourly electricity price and the related statistical distribution vector for the central air source heat pump.

The operational cost for the optimum case is calculated for the whole period as well as the benchmark system without any optimization. This can show a 4 % reduction in operation costs due to optimizing the network temperature. This reduction is the index for the importance of optimization in such systems, and this can lead to nearly 100000 USD savings in the annual expenses of the proposed district energy system. If the system has a lifespan of 20 years, we can estimate the total long-term savings to be 2 million USD. The long-term impact of the optimum case can be substantial because it provides consistent savings annually, and over time, these savings could lead to significant financial benefits. Additionally, the reduced electricity consumption makes the economy of the project less prone to risks associated with fluctuating energy prices.

In the second part, the system is to be connected to a lake with a constant temperature of 7 °C by a water source heat pump rather than the variable temperature of the ambient by an air source heat pump. In this situation, the heat source temperature would be set constant, and a water source heat pump would have the responsibility of heat transfer between the lake and the network. For this case, the optimization process for the determination of optimal network temperature is repeated, and the results are presented in Figure 6. It could be observed that in over 75% of cases, the optimum temperature of the network is calculated to be 11 °C. Interestingly, from the air source heat pump application in which the optimal network temperature of 11 °C has been repeated for 28% of cases, a 48% increase has occurred in the number of hours in which the optimal temperature of the network has been calculated to be 11 °C in water source heat pump application of the central station.

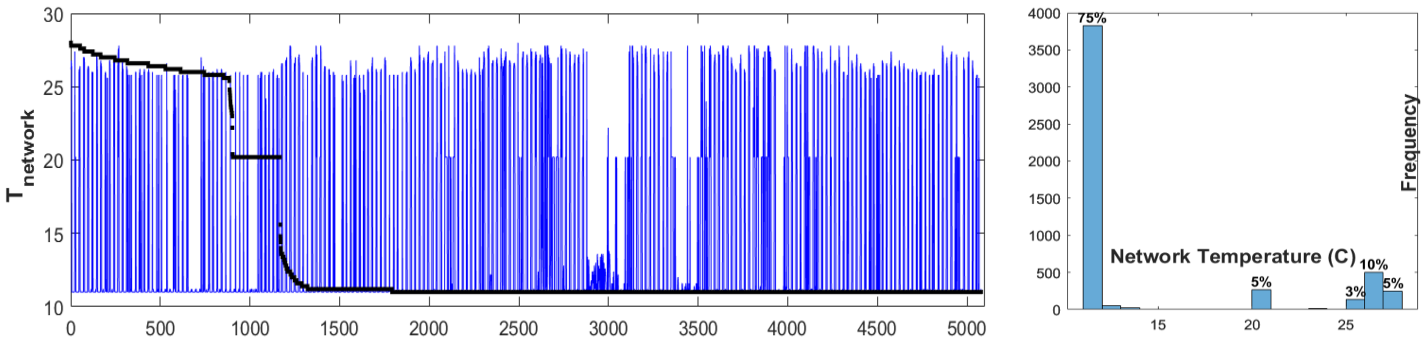

Fig. 6: Optimum network temperature and the related statistical distribution vector for the central water source heat pump.

To have a better perspective about the results, the frequency distribution of the demand and ambient temperature for when the optimal network temperature is 11 °C should be compared with the whole range of data. In Figure 7, the left plot shows the frequency distribution of the total demand across the entire dataset. The brown bars show the demand only for the case where the network temperature is 11°C. Most of the selected demands are between 2000 and 4000 kWh. This indicates that 11°C corresponds to typical or balanced demand conditions. The frequency distribution of ambient temperatures for all ambient temperatures and those ambient temperatures corresponding to the specified range of 11°C is aligned, while the frequency distribution of demands is not aligned for these two cases. The reason behind this is that the temperature of the heat source is constant and is about 7 °C, and the ambient temperature in more than 50 % of cases is around this temperature. So, there is a very good overlap between the heat source temperature and the ambient temperature. In addition, it could be observed that when the temperature of the ambient is in the range of 10 to 13 °C, for almost 100 % of cases, the optimal temperature for the network is calculated to be 11°C. It means that in this situation, the minimum temperature difference would be observed in this case between the network and the ambient. Therefore, when the ambient temperature is in the range of 10 to 13°C, the optimal network temperature is not a function of demand anymore. While in the most repeated temperature range between 3 and 7 °C, about 70 % of cases, the optimal temperature is considered to be 11 °C. We can see the distribution of the demand for this case, where the range of demand is seen to start from 1250 kWh and finish at 4750 kWh.

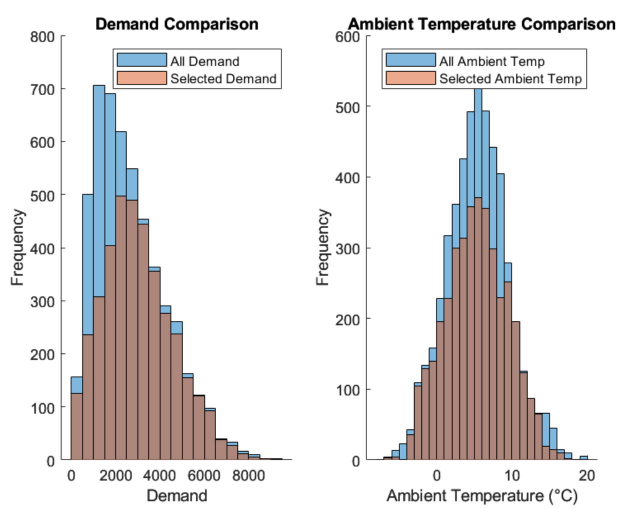

Fig. 7 Optimum network temperature and the related statistical distribution vector for the central water source heat pump.

5. Conclusion

The district heating system utilizing CO_2 as the working fluid is considered for further investigation under optimal operation conditions with respect to the temperature of the network. The significance of this operation lies in its potential to reduce the final cost of energy for end users. As the technology is still in its early stages, achieving technical feasibility is the priority. However, once implemented, the system's ability to deliver lower-cost energy and improve affordability will be crucial, both for widespread adoption and for attracting potential investment. In this study, the optimal temperature of the network is calculated for two cases, in which the heat source of the network is defined as being connected to a water source or an air source heat pump. The impact of the temperature stability of the heat source when using the water source heat pump on the central station is that there has been a 48% increase in the number of hours when the optimal network temperature is calculated to be 11 °C. In addition, this study demonstrates that the proposed optimal model for the air source heat pump at the central station improves energy cost by 4% compared to the benchmark system without any optimization. This work displayed how optimization could help in the reduction of expenses just by adjusting the proper temperature for the network.

Acknowledgements

This article comes out of the CO2inloop project which has received funding in the framework of the joint programming initiative ERA-Net GEOTHERMICA and Smart Energy Systems, with support from the European Union's Horizon 2020 research and innovation program as well as from the under the ERANET scheme of the Horizon Europe program, financially supported by Innovation Fund Denmark (Case Number: 1158-00010B) and the Austrian Research Promotion Agency (FFG)

The authors would like to express their gratitude to the project CO2inloops's team members for their invaluable support and contributions.

References

[1] Intergovernmental Panel on Climate Change, "Mitigation Pathways Compatible with 1.5°C in the Context of Sustainable Development," in Global Warming of 1.5°C: IPCC Special Report on Impacts of Global Warming of 1.5°C above Pre-industrial Levels in Context of Strengthening Response to Climate Change, Sustainable Development, and Efforts to Eradicate Poverty, Cambridge University Press, 2022, pp. 93–174. doi: 10.1017/9781009157940.004.

[2] International Energy Agency, "Net Zero by 2050," Oct. 2021.

[3] S. Buffa, M. Cozzini, M. D'Antoni, M. Baratieri, and R. Fedrizzi, "5th generation district heating and cooling systems: A review of existing cases in Europe," Renew. Sustain. Energy Rev., vol. 104, pp. 504–522, Apr. 2019, doi: 10.1016/j.rser.2018.12.059.

[4] C. Weber and D. Favrat, "Conventional and advanced CO2 based district energy systems," Energy, vol. 35, no. 12, pp. 5070–5081, 2010, doi: 10.1016/j.energy.2010.08.008.

[5] S. Henchoz, P. Chatelan, F. Maréchal, and D. Favrat, "Key energy and technological aspects of three innovative concepts of district energy networks," Energy, vol. 117, pp. 465–477, Dec. 2016, doi: 10.1016/j.energy.2016.05.065.

[6] S. Henchoz, C. Weber, F. Maréchal, and D. Favrat, "Performance and profitability perspectives of a CO2 based district energy network in Geneva's City Centre," Energy, vol. 85, pp. 221–235, Jun. 2015, doi: 10.1016/j.energy.2015.03.079.

[7] C. Weber and D. Favrat, "Conventional and advanced CO2 based district energy systems," Energy, vol. 35, no. 12, pp. 5070–5081, 2010, doi: https://doi.org/10.1016/j.energy.2010.08.008.

[8] S. Henchoz, C. Weber, F. Maréchal, and D. Favrat, "Performance and profitability perspectives of a CO2 based district energy network in Geneva's City Centre," Energy, vol. 85, pp. 221–235, Jun. 2015, doi: 10.1016/j.energy.2015.03.079.

[9] R. Pedersen, J. Worm, L. Reinholdt, B. Elmegaard, and A. Arabkoohsar, "EVALUATION OF A DISTRICT COOLING NETWORK USING R-744 AS THE ENERGY CARRIER: A CASE STUDY," in 37th International Conference on Efficiency, Cost, Optimization, Simulation and Environmental Impact of Energy Systems (ECOS 2024), Zografos, Greece: ECOS 2024, 2024, pp. 871–882. doi: 10.52202/077185-0075.